Synthesis and Optical Properties of Type II CdTe/CdS Core/Shell Quantum Dots in Aqueous Solution via Successive Ion Layer Adsorption and Reaction

Qinghui Zeng,[†,‡] Xianggui Kong,*[,†] Yajuan Sun,[†,§] Youlin Zhang,[†,§] Langping Tu,[†,§] Jialong Zhao,[†] and Hong Zhang*[,§]

Key Laboratory of Excited State Processes, Changchun Institute of Optics, Fine Mechanics and Physics, Chinese Academy of Sciences, 16 Eastern South Lake Road, Changchun 130033, China, Graduate School of Chinese Academy of Sciences, Beijing 100039, China, and Van't Hoff Institute for Molecular Sciences, University of Amsterdam, Nieuwe Achtergracht 166, 1018 WV Amsterdam, The Netherlands

Received: December 3, 2007; Revised Manuscript Received: March 31, 2008

3-Mercaptopropionic acid stabilized CdTe/CdS core/shell quantum dots (QDs) were prepared in an aqueous solution following the synthetic route of successive ion layer adsorption and reaction. The photoluminescence quantum yield of the CdTe QDs could reach 40%, from 8% of the bare core, via the control of the shell thickness. The CdTe/CdS QDs exhibited also a significant red shift of emission and excitation peaks when the shell layer grew. The experiments revealed that the CdTe/CdS QDs evolved from type I to type II core/shell structures with the increase of the shell thickness, and the evolution process is affected by the core size, shell thickness, surface quality of the core and shell, as unraveled by steady-state and time-resolved spectroscopy. The lack of photoluminescence lifetime lengthening was ascribed to the surface influence of the shell.

Introduction

Semiconductor nanocrystals (NCs) (also called quantum dots (QDs)) hold immense promise for optoelectronic and biological/biomedical applications due to their unique optical properties, such as size-tunable photoluminescence (PL), high PL quantum yield (QY), narrow emission line width, broad absorption profile, superior photostability, and flexible solution processing.[1–3] Until now, the synthetic approach in the organic phase using trioctylphosphine(TOP)/trioctylphosphine oxide (TOPO) ligands has been one of the most mature methods for preparing highly fluorescent II−VI QDs that are insoluble in water.[4–6] The QDs must be transferred from the organic to aqueous phase via surface modification, which is a prerequisite for application in biology and biomedicine.[7–9] However, the phase transfer usually results in a significant decrease of the PL QY for the QDs and sometime the as-prepared QDs have weak water solubility and stability due to the strong polarity of water molecules. Therefore, the synthesis of water-dispersed semiconductor NCs with high PL QY is also becoming one of the rich fields of scientific endeavor.

Early aqueous CdTe QDs with a low PL QY were prepared in the presence of thioglycolic acid (TGA) as the stabilizing agent by using a reaction between Cd^{2+} and NaHTe solution.[10] These QDs were easily subjected to the photooxidation and photobleaching when used to labeling in living cells, resulting in significant PL quenching.[11] To improve the QY and photostability, epitaxial growth of an inorganic shell on the surface of CdTe QDs in aqueous solution was explored in a few research groups, similar to growing a shell of ZnS, CdS, or ZnSe on CdSe cores in organic solutions.[4,12–15] CdS is in principle a good candidate as the shell material for CdTe cores not only because its band gap (2.5 eV) is wider than that of CdTe (1.5 eV) but also because its lattice parameter mismatch (3.6%) to CdTe is relatively small compared with ZnSe (12.5%) and ZnS (16.5%).[12,16] Gao et al. observed the improvement of PL QY of TGA stabilized CdTe QDs from 8 to 85% under more than 20 days of illumination and demonstrated that a CdS shell was formed on the CdTe cores.[17] Wang et al. reported a fast synthesis of CdTe/CdS QDs with high luminescence QY by a microwave-assisted method.[18] Recently, Yang et al. synthesized highly fluorescent CdTe/CdS core/shell NCs in an aqueous solution under ultrasonic irradiation by using 1-thioglycerol as a ligand.[19] In the mean time, CdTe/CdS QDs were also prepared in organic solutions.[20–22] Despite these progresses, the effect of the CdS shell thickness on the optical properties of aqueous CdTe QDs has not yet been studied in detail.

Recently, CdTe/CdS core/shell NCs were considered to be type II QDs, in which the hole is mostly confined to the CdTe core, while the electron is mostly confined to the CdS shell due to their band offsets.[21,22] Whereas for type I QDs, both the electron and the hole are confined in the same core or shell. The experimental results and theoretical modeling have shown that the spatial separation of charge carriers in the type II QDs leads to certain novel characteristics, such as a significant red shift of the emission and a long radiative lifetime (τ_r).[23–28] It is thus very demanding to study the response of the carrier dynamics of CdTe/CdS core/shell QDs to the shell thickness in order to have a better understanding of optical properties of this system.

In this work, we have synthesized the 3-mercaptopropionic acid (MPA)-stabilized CdTe/CdS core/shell QDs in an aqueous solution adopting a route of successive ion layer adsorption and reaction (SILAR) that was originally developed by Peng to prepare CdSe/CdS NCs in organic phase.[29] The structural and optical properties were characterized and studied by transmission

* To whom correspondence should be addressed. Phone: +86-431-86176313 (X.K.); +31-20-5256976 (H.Z.). E-mail: xgkong14@ciomp.ac.cn (X.K.); h.zhang@uva.nl (H.Z.).
† Key Laboratory of Excited State Processes, Changchun Institute of Optics.
‡ Graduate School of Chinese Academy of Sciences.
§ University of Amsterdam.

10.1021/jp711395f CCC: $40.75
Published on Web 05/16/2008

electron microscopy (TEM), X-ray diffraction (XRD), and optical spectroscopy. The thickness of the CdS shell was accurately controlled by changing the stoichiometry of the injection solutions and the growth condition was optimized to obtain the maximum PL QY of CdTe/CdS QDs. In particular we have performed the experiments on the thickness effect of CdS shell on the PL dynamics of CdTe/CdS QDs. Finally the photoirradiation experiment was carried out to examine the high photostability of as-prepared CdTe/CdS QDs.

Experimental Section

Chemicals. Tellurium powder (99.8%) and cadmium perchlorate hydrate ($Cd(ClO_4)_2 \cdot 6H_2O$) were purchased from Aldrich. MPA (98%) was obtained from Acros. Sodium borohydride ($NaBH_4$) and $Na_2S \cdot 9H_2O$ was obtained from Tianjin Guangfu Chemical Reagents Institute. All the reagents were used without further purification.

Synthesis Procedure of CdTe QDs. The QDs synthesis is described in detail as follows: The molar ratio of Cd:Te:MPA was settled as 1:0.25:2.4. Briefly, $NaBH_4$ was used at higher molar ratio to react with Te in water under stirring and continuously flowing of Ar at about 40 °C until a clear solution was obtained to prepare sodium hydrogen telluride (NaHTe). $Cd(ClO_4)_2 \cdot 6H_2O$ and MPA were dissolved in 25 mL of Ar-saturated deionized water followed by adjusting the solution to pH 10 with addition of 1 mol/L NaOH. Then the NaHTe solution was added to 25 mL of the above precursor solution and the complex solution with a faint yellow color was put into a Teflon-lined stainless steel autoclave with a volume of 50 mL. The autoclave was maintained at the reaction temperature for a designed time and then cooled down to room temperature by a hydrocooling process. Different-sized CdTe QDs were prepared by varying the synthesis time. The obtained CdTe QDs were precipitated by adding methanol for a deeper purification and were centrifuged at 6000 r/min. The sediment was redissolved and settled as the stock solution for the preparation of CdTe/CdS QDs.

Injection Solutions. The cadmium injection solution (0.03 M) was prepared by dissolving $Cd(ClO_4)_2 \cdot 6H_2O$ and MPA in aqueous solution with the molar ratio MPA:Cd of 2.4. The pH value was adjusted with 1 M NaOH to pH 10−11. The sulfur injection solution (0.025 M) was prepared by dissolving $Na_2S \cdot 9H_2O$ in aqueous solution. For the sake of faster contacting of cations onto the surface of CdTe core than the anions, the concentration of cadmium injection solution was set to be a little higher than that of the sulfur injection solution. Both injection solutions were made under an Ar flow at room temperature. For each injection, a calculated amount of a given injection solution was taken with a syringe at the speed of 0.2 mL/2 min.

A SILAR Synthetic Procedure of CdTe/CdS Core/Shell QDs. CdTe (20 mL, 0.1 mmol/L) QDs were added to a three-necked flask and stirred under Ar flowing for 1 h. Then the CdTe stock solution was heated up to the desired temperatures and the injection solutions were dropped into the solution at the speed of 0.2 mL/2 min. The amount of Cd and S precursors required for each layer was determined by the number of the surface atoms of a given size of a core/shell QDs. The average thickness of one monolayrer of CdS was taken as 0.35 nm according to the method developed by Peng et al.[29] The concentration of CdTe QDs was estimated from the reported extinction coefficient per mole of particles (ϵ)[30] by using Lambert−Beer's law. As a result, the diameter of the one monolayer passivated CdTe QDs would be increased for 0.7 nm. For example, in a typical experiment with 2 μmol of 1.5 nm CdTe core, 2.8 mL of Cd and S precursors is needed for the first layer of the shell growth, and additional 3.6 mL of Cd and S precursors completes the growth of the second layer, and 5.0 mL of Cd and S precursors completes the growth of the third layer, and 6.2 mL of Cd and S precursors completes the growth of the fourth layer, and so forth.

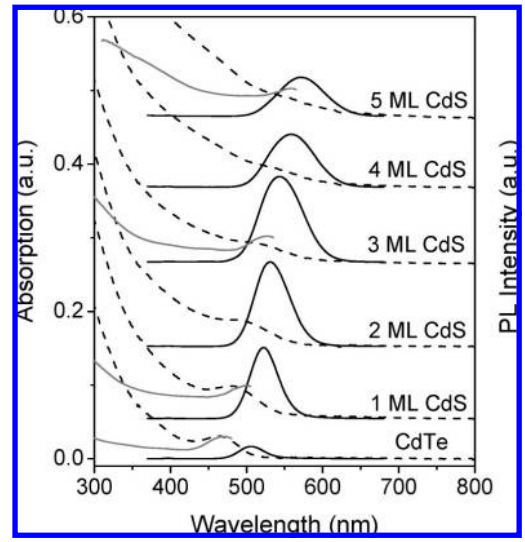

Figure 1. Absorption (dashed lines), PL (solid lines), and excitation (gray solid lines) spectra of the CdTe/CdS core/shell QDs. The shell thicknesses are given in the figure.

Apparatus. Ultraviolet−visible (UV−vis) absorption and fluorescence spectra were measured at room temperature by a UV-3101 spectrophotometer and a Hitachi F-4500 fluorescence spectrofluorimeter, respectively. Unless claimed otherwise, the excitation wavelength was set at 350 nm. The optical densities (ODs) at the excitation wavelength for the reference dye and the QDs were set to be identical for QY determination. The OD at the first exciton absorption peak of the QDs was adjusted to be less than 0.05 in order to avoid any significant reabsorption. The QY of nanocrystal solutions was determined by using Rhodamine 6G in ethanol as a standard. The sizes of CdTe QDs were either determined by a TEM (JEOL-3010) or calculated with the wavelength of the first excitonic absorption peak.[30] Power X-ray diffraction (XRD) patterns were recorded on a Rigaku D/MAXIIA diffractometer using Cu Kα radiation. Fluorescence lifetimes were measured using the time-correlated single photon counting technique with FL920-fluorescence lifetime spectrometer (Edinburgh instrument) with the instrument response of ~1 ns. The excitation source was an nF900 ns flash lamp. The recorded decay curves were fitted with a multiexponential function deconvoluted with the system response. The photoirradiation experiments were performed under ambient condition and irradiation from a 365-nm ultraviolet lamp at certain time intervals. The samples were prepared by the 1:200 dilution of a stock solution.

Results and Discussion

Figure 1 shows the absorption and PL spectra of 1.5-nm CdTe core QDs with various thicknesses of CdS shell. As readily seen in Figure 1, a strong luminescence band is observed near the band edge and no deep trap luminescence is detected, indicating the decent emissive properties of the QDs.[31−33] The PL intensity of the QDs increases with the growth of the CdS shell on CdTe cores from 1 to 3 monolayers (MLs) and then

declines when the shell continues to grow from 3 to 5 MLs. A significant red shift of emission appears upon the increase of the CdS shell thickness, e.g., PL is peaked at 522.2 nm for 1 ML and at 570.8 nm for 5 MLs. On top of that, the first exciton peak in the absorption spectra shifts to longer wavelength and disappears gradually with the shell thickness becoming thicker. The smearing of the exciton absorption peak was taken as the feature of type II QDs.[23,26–28,34] In general, the optical spectroscopy of CdTe QDs with a CdS shell is determined by the following factors: (1) transition between the electron of CdS shell and the hole of CdTe core, (2) transition between the electron and hole of CdTe cores, and (3) size distribution of the QDs. To sort out the influence of the absorption broadening originated from other species not contributing to the observed emission, PL excitation (PLE) spectra were measured by monitoring the PL at peak wavelength and typical PLE spectra are included in Figure 1 as well. The first exciton band distinctly appears in the PLE, in contrary to the absorption spectra of thick shell samples. The maximal red shift achieved in our experiment is around 65 nm when one compares 1.5-nm bare CdTe with the one coated with a 5-ML CdTe shell. At the first instance this value seems relatively small. However one should bear in mind that the offset between the conduction bands of the CdTe core and CdS shell is small, i.e., ~0.1 eV for their bulk counterparts, much less than that of other systems, e.g., the valence band offset of CdS and ZnSe is ~0.52 eV.[27] Such a small difference in conduction band offset between the core and shell is responsible for the observed "small" red shift in PLE and PL. The almost unchanged difference between the PLE peak and PL maximum manifests itself the impossibility of distinguishing the type I and type II emission by simply looking at the Stokes shift for such a case due to the existence of various factors (vide supra). The relation between the two type structures and the shell thickness can be visualized as follows: When the shell thickness is relatively thin, the core quantum well gets larger compared with the situation of bare core and the first electron and hole levels will get closer in energy, correspondingly. While hole wave function is still confined in the quantum well of the core, electron wave function spreads over the core and shell, so-called quasi type II structure.[27] Here the system behaviors like a mixture of type I and type II QDs. When the shell gets even thicker, electron wave function will be confined mainly in the shell whereas hole wave function remains in the core. In this case typical type II behavior should appear. To verify the hypothesis, we have performed detailed analysis on the steady-state and time-resolved optical spectroscopy.

The QY and full width at half maximum (fwhm) of the PL spectra of CdTe/CdS core/shell QDs with different shell layers are depicted for 1.5-nm CdTe core in Figure 2. The PL QY is significantly enhanced to maximal value of 40 from 8% of the bare cores by growing a CdS shell on CdTe core. The QY reaches the maximum when the shell thickness is around 3 MLs and then decreases rapidly with the shell growth from 3 to 5 MLs. This phenomenon can be related to several factors. When a thin shell layer, i.e., less than 3 MLs, presents the PL QY of CdTe/CdS QDs the passivation of the core surface, the shell layer will reduce the PL quenching centers and hence improve the PL QY. In this case the system is in quasi type I structure where the electron−hole recombination occurs mainly in the core, i.e., the transition moment does not change much from that of bare core. Therefore the surface passivation plays a dominant role. Further increase of the shell thickness results in the decline of the QY, which indicates that other mechanisms play a role as well. For type I core/shell QDs, similar

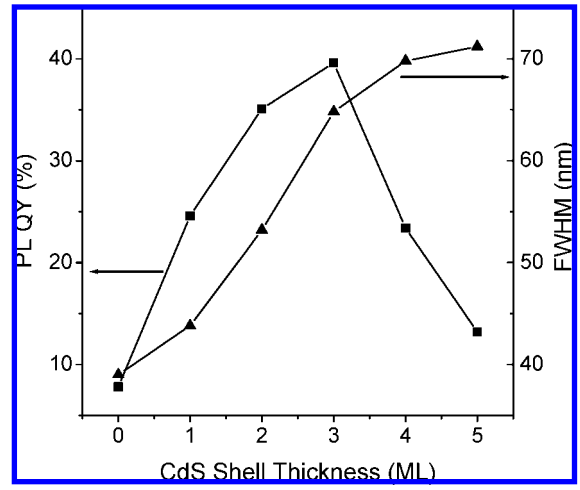

Figure 2. The QY and fwhm of the CdTe QDs with different layers of CdS shell. The CdTe core is 1.5 nm in diameter.

observations were ascribed to the strain released through the formation of dislocations in the shell with increasing shell thickness, e.g., CdSe/ZnS core/shell system.[13,35,36] However, when a core/shell system evolves from type I to type II structure the electron−hole recombination process, which is responsible for the PL, will also change from direct recombination to indirect recombination. Such a change, in general, leads to the decline of the QY.[24] In the mean time the surface quality of the shell shall contribute significantly to the PL because now electron wave function is confined in the shell. These two possibilities can be distinguished by PL dynamics studies (vide infra). Furthermore, it is noted that the bandwidth of the emission increases with increasing the shell thickness, which is different from the situation of type I CdSe/CdS QDs, where the PL line width demonstrates independence of the shell thickness.[29]

To characterize the quality of the samples, typical TEM and high-resolution (HR) TEM images of CdTe cores and corresponding core/shell QDs with different CdS shell thickness are shown in Figure 3. As seen from parts A to C of Figure 3, the diameter of the QDs with nearly spherical shape becomes larger with the shell growth. The interfacial layer is not observed in the HRTEM images due to the high lattice match between the core and shell materials, indicating the coherent epitaxial growth of CdS shell along the lattice planes of the CdTe core.[18] Size histogram of the CdTe QDs is shown in Figure 4. The diameters of the particles were determined to be 1.5 nm for the CdTe cores and 3.3 and 4.8 nm after the CdTe cores were covered with the designed CdS shells of 3 and 5 MLs, respectively. These data are in good agreement with the theoretical values calculated from the amount of injected solutions when the thickness of 1 ML of CdS shell was estimated to be about 0.35 nm. This, in turn, proves that the shell thickness of CdTe/CdS QDs can be well controlled by the SILAR technique.

The XRD patterns of MPA-stabilized CdTe cores and CdTe/CdS core/shell QDs with different shell thickness are presented in Figure 5. The diffraction pattern of the bare CdTe core QDs is consistent with that of bulk cubic CdTe structure, while the diffraction pattern of CdTe/CdS QDs moves gradually toward higher angle with increasing the shell thickness. No distinct peak was observed from CdS, similar to the formation of CdS shell on CdTe core reported previously.[17–19] However, caution should be taken here in drawing conclusion because such an XRD pattern can correspond to either CdS_xTe_{1-x} alloy or CdTe/CdS core/shell nanocrystals.[18] To this end it is recalled that CdS_xTe_{1-x}

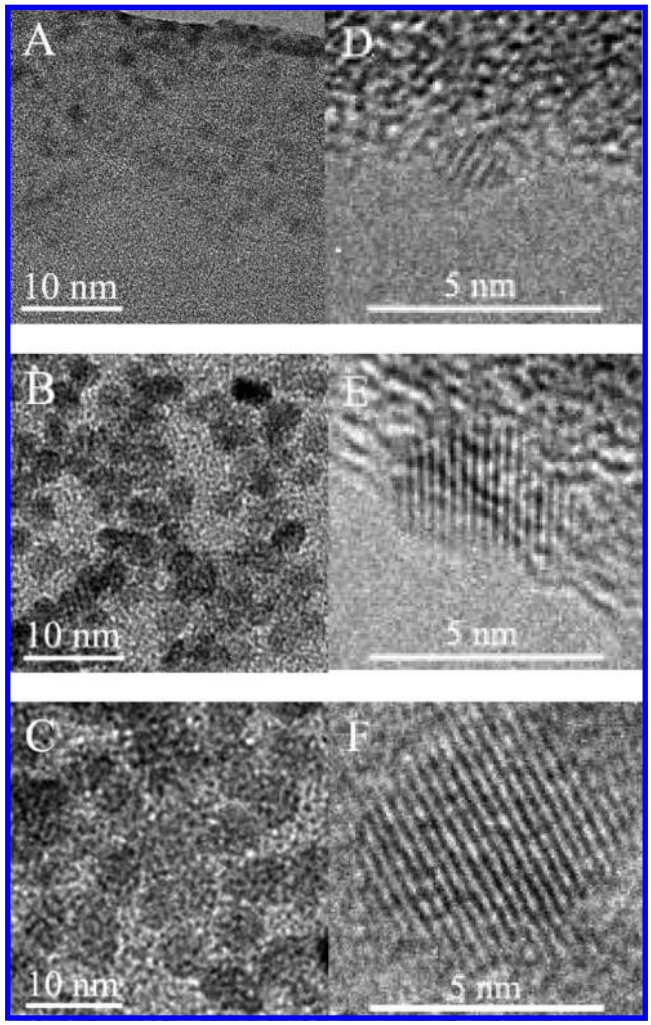

Figure 3. TEM images of CdTe/CdS QDs with different shell thickness. (A) and (D) CdTe cores; (B) and (E) plus 3 MLs of CdS; (C) and (F) plus 5 MLs of CdS.

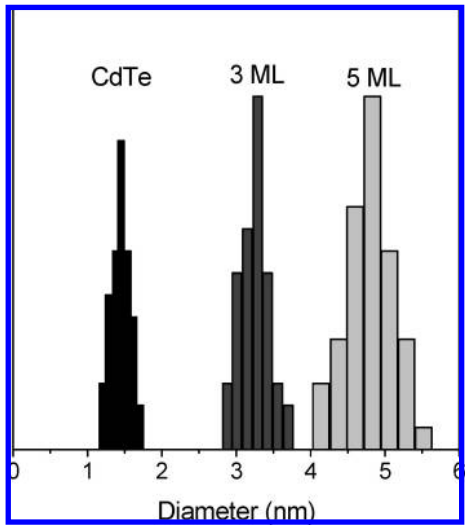

Figure 4. Size histogram for the CdTe core/shell QD samples used in Figure 3.

alloy nanocrystals, e.g., formed via substitution of tellurium atoms with sulfur, would result in a blue shift of absorption and PL spectra because of the larger energy band gap of CdS_xTe_{1-x} compared to pure CdTe.[18,37] Therefore the observed

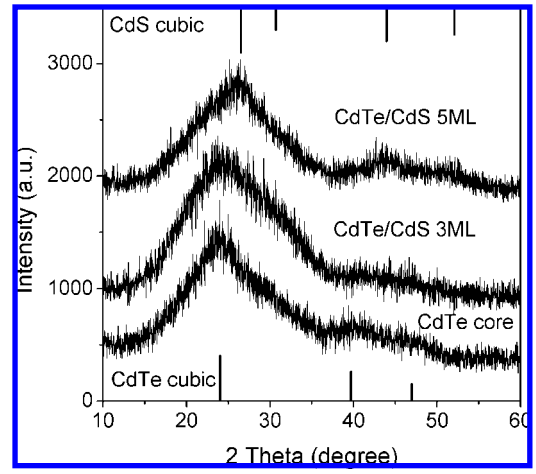

Figure 5. XRD patterns of CdTe and CdTe/CdS core/shell QDs.

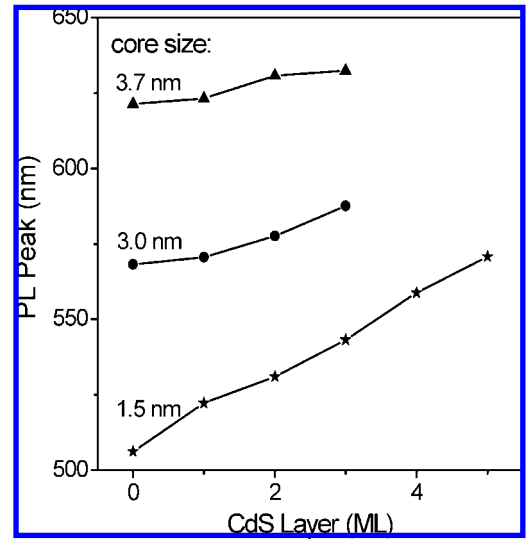

Figure 6. PL peak positions of CdTe core/shell QDs with different layers of CdS shell.

red shift in both the emission and absorption spectra in this case is a strong evidence for the formation of CdTe/CdS core/shell QDs.

Figure 6 shows the emission peaks for different-sized CdTe/CdS QDs as a function of CdS shell thickness. Because the aggregation occurs for large-sized core/shell QDs, we could not obtain the CdTe/CdS core/shell QDs with a shell thicker than 3 MLs for large QDs. As seen from Figure 6, the PL peak shifts to longer wavelength when the CdS shell is grown on the CdTe core. Compared with the emission of CdTe cores, the red shifts of 3 ML CdTe/CdS core/shell QDs with core sizes of 3.7, 3.0, and 1.5 nm were determined to be 11.0, 19.4, and 37.4 nm, respectively. The red shift increasing with the core size decreasing is due to the quantum size effect of CdTe cores. For type I QDs the small red shift was considered to originate from the spreading of the electronic wave functions into the shell, which was strongly dependent on the shell material.[5,12,13,35,36] The origin of the red-shift of type II CdTe/CdS QDs is, however, different.

Recently CdTe/CdS core/shell NCs were considered as type II QDs, in which the energy level of the conduction band in the CdTe shell is estimated to be about 0.1 eV slightly higher than that in CdS shell based on the band offsets of the bulk materials.[21,22] The energy level diagram of CdTe/CdS QDs with a diameter of 1.5 nm is shown in Figure 7. For the bare CdTe

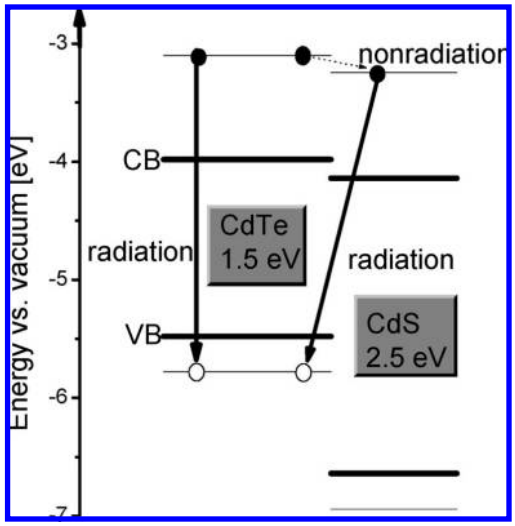

Figure 7. Schematic energy diagram of the CdTe/CdS core/shell QDs. Bold and thin lines represent the VB and CB of the bulk material and QDs, respectively. The solid and dot arrows represent the radiation and nonradiation processes, respectively.

cores, the luminescence band near the band gap as shown in Figure 1 is often considered to come from recombination of excitons in CdTe. We hypothesize that CdTe/CdS core/shell QD will gradually evolve into a type II core/shell structure from a type I CdTe core with increasing CdS shell thickness. As seen in Figure 7, for the CdTe/CdS QDs with a CdS shell, both type I (recombination of an electron and hole in CdTe core) and type II (recombination of an electron in CdS and a hole in CdTe) mechanisms coexist, which causes a broadening of the PL band, as well as a significant red shift and a long radiative lifetime.[24,28] Furthermore, the PL from the type II QDs will become dominant with the increase of the CdS shell thickness although we could not distinguish the origin of the emission in the spectrum perhaps because of a small energy difference between conduction bands of CdTe and CdS.[21,22] This is consistent with the fact that the red shift of the PL spectra between the core and core/shell QDs obtained above is not as substantial as other typical type II core/shell QDs.[23–25,27]

It is noted that many reports are on the study of PL decays of CdTe cores,[31–33,38] but few are on the CdTe/CdS core/shell QDs.[21] The reported nonexponential decay times spread over an extremely broad range from a few hundreds of picoseconds to a few hundreds of nanoseconds. The variation of the PL decay lifetimes was suggested to be strongly dependent on the surface chemistry of CdTe NCs.[38,39]

Figures 8 and 9 show the PL decay curves of 1.5- and 3.0-nm CdTe/CdS core/shell QDs with different shell thickness. As seen clearly in Figures 8 and 9, the dynamics of photogenerated carriers is not single exponential for bare CdTe cores and the core/shell QDs. The time decays can be well fitted with a biexponential model described by $I(t) = B_1 \exp(-t/\tau_1) + B_2 \exp(-t/\tau_2)$, where τ_1 and τ_2 represent the time constants and B_1 and B_2 represent the amplitudes of the components, respectively.[33] The average lifetime τ is calculated by an expression $\tau = (B_1\tau_1^2 + B_2\tau_2^2)/(B_1\tau_1 + B_2\tau_2)$. The fitting parameters B_1, B_2, τ_1, τ_2, τ, and τ_r are summarized in Table 1. The fast component of the PL decay in bare CdTe cores can be attributed to an exciton recombination. However, the origin of the slow component in the CdTe cores is not clear. The long PL decay in CdSe cores is considered to originate from the surface-related emission or the emission of dark excitons.[40,41] As can be clearly seen in Table 1, with increasing the CdS shell thickness the

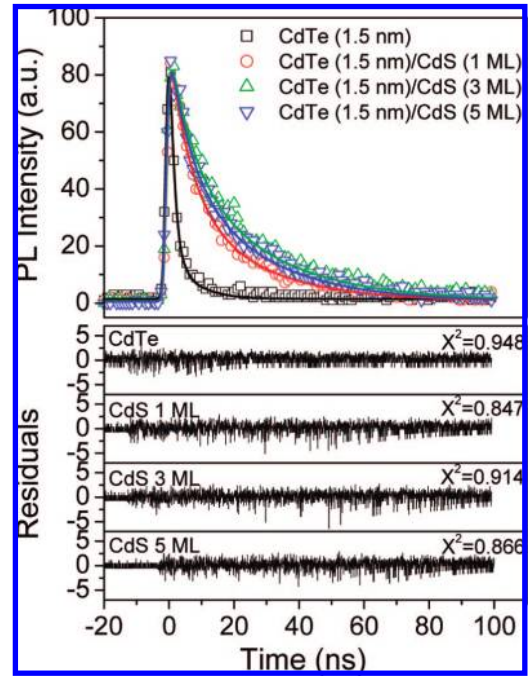

Figure 8. The luminescence decay curves of CdTe/CdS QDs with core size of 1.5 nm. The excitation wavelength is 350 nm. The lower panel shows weighted residuals for biexponential fits.

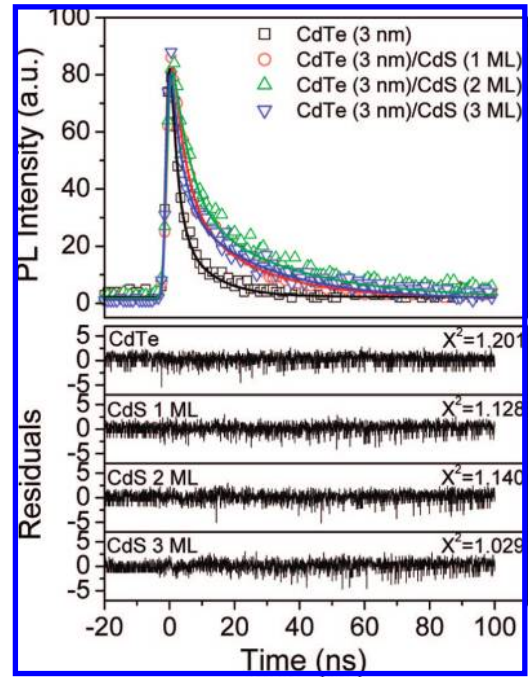

Figure 9. The luminescence decay curves of CdTe/CdS QDs with core size of 3.0 nm. The excitation wavelength is 350 nm. The lower panel shows weighted residuals for biexponential fits.

fast component (B_1%) of the PL decay for CdTe/CdS QDs decreases while the slow component (B_2%) increases. In contrast to that of the bare cores, the average PL decay time of the core/shell QDs is found to be greatly lengthened. The average PL decay lifetime of 1.5-nm CdTe core QDs was found to increase from 3.5 ns to 18.0 (with 1 ML CdS shell) and 22.7 ns (with 3 ML CdS shell), respectively. The PL decay time decreases to 19.0 ns when the shell thickness reaches 5 MLs. This lifetime lengthening for thin shell and shortening again for thicker shell might be related to two mechanisms. On the one hand, the nonradiative channels can be modified by the surface capping

TABLE 1: PL QY, Time Constants τ_1 and τ_2, Components B_1% and B_2% of τ_1 and τ_2, Average Lifetime τ and the Radiative Lifetime of the Different-Sized Core and Core/Shell QDs

sample	QY (%)	B_1%	τ_1 (ns)	B_2%	τ_2 (ns)	τ (ns)	τ_r (ns)
CdTe (1.5 nm)	7.8	63%	1.3	37%	7.3	3.5	44.9
CdTe/CdS (1 ML)	24.6	26%	5.8	74%	22.2	18.0	73.2
CdTe/CdS (3 ML)	39.6	18%	6.7	82%	26.1	22.7	57.3
CdTe/CdS (5 ML)	13.2	19%	6.1	81%	24.2	19.0	143.9
CdTe (3 nm)	9.9	45%	2.0	55%	10.3	6.5	65.7
CdTe/CdS (1 ML)	23.4	29%	3.6	71%	21.4	16.3	69.7
CdTe/CdS (2 ML)	34.6	27%	5.1	73%	30.6	23.6	68.2
CdTe/CdS (3 ML)	28.4	22%	3.2	78%	25.6	20.8	73.2

of organic molecules and surface passivation of inorganic shells,[42] which will cause the lengthening of luminescence lifetime. On the other hand, when the shell gets thicker, the system will gradually evolve from type I to type II QDs and now electrons will be located more and more in the shell. Therefore the shell structure will influence the exciton recombination process. Since in this case the surface of the shell is not passivated, there must be a plenty of luminescence quenching centers, which will result in the shortening of the lifetime of the electrons and hence the luminescence lifetime. This mechanism might be responsible for the lack of luminescence lifetime lengthening.

It is known that hole is mostly confined to the core, while the electron is mostly confined to the shell in type II CdTe/CdS QD structure.[21,22] The spatial separation of electron and hole will result in a decrease of the wave function overlap and thus longer radiative lifetime. Hence, the radiative lifetime has been predicted to be strongly dependent on the shell thickness and to increase with increasing the shell thickness.[23–28] We estimated the radiative lifetime of the QDs using the relation $QY = k_r/(k_r + k_{nr})$ and $1/\tau = k_r + k_{nr}$. The radiative lifetime for the small CdTe/CdS QDs with a core diameter of 1.5 nm was increased gradually from 44.9 ns for bare core to 143.9 ns for 5 ML shell, which is consistent with the predicted property of type II core/shell QDs. Interestingly, τ_r of the large QDs with a core diameter of 3.0 and 3.7 nm demonstrates much less dependence of the shell thickness, which reflects more type I behavior. This result can be rationalized by the fact that quantum confinement energy of electron is proportional to $1/D^2$, where D is the diameter of the QDs. Therefore the bigger the core the less sensitive it will be on the shell thickness during the evolution from type I to type II. The critical shell thickness to come into type II structure depends also on the core size. The larger the core the larger the critical shell thickness is, which leads to less quantum confinement and in turn less Stokes shift in PL.

Therefore, the transition between CdTe/CdS core/shell QDs from type I to II can be realized in principle by tuning the size of CdTe core or changing the shell thickness. Furthermore, the nonradiative decay rate, k_{nr}, of the QDs was obtained by $k_{nr} = (1 - QY)/\tau$. Accordingly, the nonradiative decay rates were decreased from 2.63×10^8 s^{-1} for 1.5 nm CdTe core to 4.19×10^7, 2.66×10^7 s^{-1}, and then increased to 4.57×10^7 s^{-1}, for CdTe/CdS core/shell QDs with CdS shells of 1, 3, and 5 MLs, respectively. Similarly, the nonradiative decay rates were decreased from 1.39×10^8 s^{-1} for 3 nm CdTe core to 4.70×10^7, 2.77×10^7, and then increased to 3.44×10^7 s^{-1} for CdTe/CdS QDs with CdS shells of 1, 2, and 3 MLs, respectively. As a result, the nonradiative decay rate might be related to unpassivated surface of the CdS shell, leading to the lack of systematic lengthening in PL lifetime of CdTe/CdS core/shell QDs with the increase of the shell thickness.

The optical properties of CdTe/CdS QDs under continuous irradiation were also studied to illustrate the photostability of the core/shell structures. It is known that the PL QY of QDs decreases with time under ultraviolet light irradiation due to photo-oxidation reaction.[43] In our experiment, no significant blue shift of the emission from the photo-oxidation was observed in the CdTe/CdS core/shell QDs with CdS shell of 3 MLs for the same illumination time (4 h), which makes CdTe/CdS core/shell QDs a promising candidate for applications in biology/biomedicine imaging and detection.

Conclusions

In summary, we adopted the SILAR technique to synthesize MPA stabilized CdTe/CdS core/shell QDs in aqueous phase, where the growth of CdS shell was properly controlled. The luminescence QY of CdTe/CdS core/shell QDs was enhanced from 8% of the bare core up to 40% after the surface passivation by a CdS shell of optimal thickness. The luminescence of the CdTe/CdS QDs came not only from the recombination between an electron of CdS shell and a hole of CdTe core but also from the recombination between an electron and a hole confined in CdTe core. The shell thickness-dependent photoluminescence decay and QY were related to surface passivation of the core and surface traps of the shell. The two processes jointly determined the PL decay behavior. The lengthening of the radiative lifetime was confirmed in CdTe/CdS QDs with the increase of the CdS shell thickness, indicating the evolution of CdTe/CdS QDs from type I to type II structure.

Acknowledgment. This work was supported by NSFC of China (60771051, 60601014, and 20603035), the National High Technology Development Program (2006AA03Z335), the Major Foundation of Chinese Academy of Sciences (kjcx2-sw-h12-02), and exchange program between CAS of China and KNAW of The Netherlands. J.Z. gratefully acknowledges the support of the K.C. Wong Education Foundation, Hong Kong.

References and Notes

(1) Colvin, V. L.; Schlamp, M. C.; Alivisatos, A. P. *Nature* **1994**, *370*, 354.
(2) Bruchez, M. J.; Moronne, M.; Gin, P.; Weiss, S.; Alivisatos, A. P. *Science* **1998**, *281*, 2013.
(3) Chan, W. C. W.; Nie, S. M. *Science* **1998**, *281*, 2016.
(4) Murray, C. B.; Norris, D. J.; Bawendi, M. G. *J. Am. Chem. Soc.* **1993**, *115*, 8706.
(5) Peng, X. G.; Schlamp, M. C.; Kadavanich, A. V.; Alivisatos, A. P. *J. Am. Chem. Soc.* **1997**, *119*, 7019.
(6) Peng, Z. A.; Peng, X. G. *J. Am. Chem. Soc.* **2001**, *123*, 183.
(7) Jaiswal, J. K.; Mattoussi, H.; Mauro, J. M.; Simon, S. M. *Nat. Biotechnol.* **2003**, *21*, 47.
(8) Guo, W. Z.; Li, J. J.; Wang, Y. A.; Peng, X. G. *J. Am. Chem. Soc.* **2003**, *125*, 3901.
(9) Kim, S.; Bawendi, M. G. *J. Am. Chem. Soc.* **2003**, *125*, 14652.
(10) Rogach, A. L.; Katsikas, L.; Kornowski, A.; Su, D.; Eychmuller, A.; Weller, H. *Ber. Bunsen−Ges. Phys. Chem.* **1996**, *100*, 1772.
(11) Zhang, Y.; He, J.; Wang, P. N.; Chen, J. Y.; Lu, Z. J.; Lu, D. R.; Guo, J.; Wang, C. C.; Yang, W. L. *J. Am. Chem. Soc.* **2006**, *128*, 13396.
(12) Hines, M. A.; Guyot-Sionnest, P. *J. Phys. Chem.* **1996**, *100*, 468.
(13) Dabbousi, B. O.; Rodriguez-Viejo, J.; Mikulec, F. V.; Heine, J. R.; Mattoussi, H.; Ober, R.; Jensen, K. F.; Bawendi, M. G. *J. Phys. Chem. B* **1997**, *101*, 9463.
(14) Danek, M.; Jensen, K. F.; Murray, C. B.; Bawendi, M. G. *Chem. Mater.* **1996**, *8*, 173.
(15) Reiss, P.; Bleuse, J.; Pron, A. *Nano Lett.* **2002**, *2*, 781.
(16) Trindade, T.; Brien, P. O.; Pickett, N. L. *Chem. Mater.* **2001**, *13*, 3843.
(17) Bao, H. B.; Gong, Y. J.; Li, Z.; Gao, M. Y. *Chem. Mater.* **2004**, *16*, 3853.

(18) He, Y.; Lu, H. T.; Sai, L. M.; Lai, W. Y.; Fan, Q. L.; Wang, L. H.; Huang, W. *J. Phys. Chem. B* **2006**, *110*, 13370.
(19) Wang, C. L.; Zhang, H.; Zhang, J. H.; Li, M. J.; Sun, H. Z.; Yang, B. *J. Phys. Chem. C* **2007**, *111*, 2465.
(20) Schreder, B.; Schmidt, T.; Ptatschek, V.; Winkler, U.; Materny, A.; Umbach, E.; Lerch, M.; Muller, G.; Kiefer, W.; Spanhel, L. *J. Phys. Chem. B* **2000**, *104*, 1677.
(21) Scho1ps, O.; Thomas, N. L.; Woggon, U.; Artemyev, M. V. *J. Phys. Chem. B* **2006**, *110*, 2074.
(22) Chang, J. Y.; Wang, S. R.; Yang, C. H. *Nanotechnology* **2007**, *18*, 345602.
(23) Kim, S.; Fisher, B.; Eisler, H. J.; Bawendi, M. G. *J. Am. Chem. Soc.* **2003**, *125*, 11466.
(24) Chen, C. Y.; Cheng, C. T.; Yu, J. K.; Pu, S. C.; Cheng, Y. M.; Chou, P. T.; Chou, Y. H.; Chiu, H. T. *J. Phys. Chem. B* **2004**, *108*, 10687.
(25) Cheng, C. T.; Chen, C. Y.; Lai, C. W.; Liu, W. H.; Pu, S. C.; Chou, P. T.; Chou, Y. H.; Chiu, H. T. *J. Mater. Chem.* **2005**, *15*, 3409.
(26) Oron, D.; Kazes, M.; Banin, U. *Phys. Rev. B* **2007**, *75*, 035330.
(27) Ivanov, S. A.; Piryatinski, A.; Nanda, J.; Tretiak, S.; Zavadil, K. R.; Wallace, W. O.; Werder, D.; Klimov, V. I. *J. Am. Chem. Soc.* **2007**, *129*, 11708.
(28) Li, J. J.; Tsay, J. M.; Michalet, X.; Weiss, S. *Chem. Phys.* **2005**, *318*, 82.
(29) Li, J. J.; Wang, Y. A.; Guo, W. Z.; Keay, J. C.; Mishima, T. D.; Johnson, M. B.; Peng, X. G. *J. Am. Chem. Soc.* **2003**, *125*, 12567.
(30) Yu, W. W.; Qu, L. H.; Guo, W. Z.; Peng, X. G. *Chem. Mater.* **2003**, *15*, 2854.
(31) Kapitonov, A. M.; Stupak, A. P.; Gaponenko, S. V.; Petrov, E. P.; Rogach, A. L.; Eychmüller, A. *J. Phys. Chem. B* **1999**, *103*, 10109.
(32) Wuister, S. F.; Koole, R.; de Mello Donega, C.; Meijerink, A. *J. Phys. Chem. B* **2005**, *109*, 5504.
(33) Osovsky, R.; Kloper, V.; Kolny-Olesiak, J.; Sashchiuk, A.; Lifshitz, E. *J. Phys. Chem. C* **2007**, *111*, 10841.
(34) Xie, R. G.; Zhong, X. H.; Basché, T. *Adv. Mater.* **2005**, *17*, 2741.
(35) Talapin, D. V.; Mekis, I.; Gotzinger, S.; Kornowski, A.; Benson, O.; Weller, H. *J. Phys. Chem. B* **2004**, *108*, 18826.
(36) Xie, R. G.; Kolb, U.; Li, J. X.; Basché, T.; Mews, A. *J. Am. Chem. Soc.* **2005**, *127*, 7480.
(37) Streckert, H. H.; Ellis, A. B. *J. Phys. Chem.* **1982**, *86*, 4921.
(38) Rogach, A. L.; Franzl, T.; Klar, T. A.; Feldmann, J.; Gaponik, N.; Lesnyak, V.; Shavel, A.; Eychmüller, A.; Rakovich, Y. P.; Donegan, J. F. *J. Phys. Chem. C* **2007**, *111*, 14628.
(39) Wuister, S. F.; de Mello Donega, C.; Meijerink, A. *J. Phys. Chem. B* **2004**, *108*, 17393.
(40) Wang, X. Y.; Qu, L. H.; Zhang, J. Y.; Peng, X. G.; Xiao, M. *Nano Lett.* **2003**, *3*, 1103.
(41) Efros, Al. L.; Rosen, M.; Kuno, M.; Nirmal, M.; Norris, D. J.; Bawendi, M. *Phys. Rev. B* **1996**, *54*, 4843.
(42) Schlegel, G.; Bohnenberger, J.; Potapova, I.; Mews, A. *Phys. Rev. Lett.* **2002**, *88*, 137401.
(43) Spanhel, L.; Haase, M.; Weller, H.; Henglein, A. *J. Am. Chem. Soc.* **1987**, *109*, 5649.

JP711395F